Two-body hadronic decays of Ξ_c^0 in light front approach

Hang Liu[1,†] and Chang Yang[1,2,*]

[1]*INPAC, Key Laboratory for Particle Astrophysics and Cosmology (MOE), Shanghai Key Laboratory for Particle Physics and Cosmology, School of Physics and Astronomy, Shanghai Jiao Tong University, Shanghai 200240, China*

[2]*Tsung-Dao Lee Institute, Shanghai Jiao Tong University, Shanghai 200240, China*

(Received 27 April 2023; accepted 14 November 2023; published 30 November 2023)

In this study, we investigate the nonleptonic decays of the charmed-baryon Ξ_c^0 induced by the $c \to u(d\bar{d})/(s\bar{s})$ transition. Utilizing the factorization assumption, we decompose the decay amplitudes in terms of transition form factors which are then calculated within the light-front quark model. We employ helicity amplitudes to analyze the nonleptonic decay modes of the charmed-baryons Ξ_c^0 and derive benchmark results for decay widths and branching fractions. Our calculations suggest that the branching fractions for some of these rare nonleptonic decays are at the order of 10^{-5}–10^{-4}, which are likely to be detectable at experiments such as LHCb, Belle-II, etc. The potential data accumulated in the future may help to further our understanding of the decay mechanism in the presence of charm quarks.

DOI: 10.1103/PhysRevD.108.093011

I. INTRODUCTION

Weak decays of quarks can provide valuable insights into testing the standard model of particle physics and advancing our understanding of CP violation in the universe. As most quarks in nature are confined within hadrons, the study of weak decays of quarks inside a hadron also provides a unique opportunity to explore strong interactions. Over the past few decades, significant progress has been made on both the experimental and theoretical fronts, resulting in unprecedentedly precise experimental measurements and theoretical calculations of hadron decays.

Both theoretical and experimental studies have shown considerable interest in the two-body hadronic decays of charmed baryons [1–12]. Experimental data on these decays have been extensively collected from various sources [13–15], while theoretical calculations have proven challenging due to the strong QCD interaction at the charm scale. Lattice QCD is believed to ultimately offer reliable theoretical results of form factors [16–21]. And several theoretical studies on these decays rely on modeling QCD dynamics to predict and test various models [22–29]. Sufficient experimental data would allow for the determination of all amplitudes classified by $SU(3)$ symmetry properties, enabling systematic predictions to further test the model and gain additional insights into strong QCD interactions at the charm scale [30–40]. The Belle collaboration [3,13,14,41,42] has accumulated the world's largest data sample of e^+e^- collision at the center-of-mass energy of around 10 GeV, and via the B meson decay chain, has access to all the lower-lying antitriplet charmed baryons. A significant recent hot topic includes the determination of absolute branching fractions for $\Xi_c^0 \to \Xi^- l^+ \nu_l$ [43], uncovering notable $SU(3)_F$ symmetry deviations [44]. Comprehensive investigations have been conducted by BESIII on the lightest charmed baryon Λ_c^+, through e^+e^- interactions at a center-of-mass energy of $\sqrt{s} = 4.6$ GeV. Should BESIII be capable of elevating the center-of-mass energy above 4.95 GeV [15,45–48], which corresponds closely to the mass of Ξ_c particle pairs, it would enable precise measurements of the absolute branching fractions for Ξ_c decays. In contrast, the LHCb collaboration [49–52] has amassed substantial datasets of charmed hadrons from proton-proton collisions at center-of-mass energies of $\sqrt{s} = 7, 8, 13$ GeV. Despite the presence of more intricate backgrounds compared to those encountered at BESIII and Belle, a majority of recent discoveries in the domain of charmed baryons, including the renowned doubly charmed baryon, have been realized at LHCb. The prompt Ξ_c^+ production cross-section in pPb and Pbp collisions at a center-of-mass energy of $\sqrt{s_{NN}} = 8.16$ TeV at the LHCb experiment is measured differentially for the first time as a function of p_T and y^* [53]. However, some experimental results for the specific processes are still missing. The purpose of this paper is to utilize the light front approach in computing the rare

*Corresponding author: 15201868391@sjtu.edu.cn
†liuhang303@sjtu.edu.cn

nonleptonic decays of Ξ_c^0, including those that have not yet been observed experimentally.

As the phase space for this class of decays is extremely limited, only a few channels are kinematically accessible. In this study, we investigate the $c \to u$ transition in the nonleptonic decays of heavy baryons Ξ_c^0, and consider explicitly

(i) the spin-1/2 to spin-1/2 decays,

$$\Xi_c^0 \to \Sigma^0\eta, \qquad \Xi_c^0 \to \Sigma^0\eta'$$
$$\Xi_c^0 \to \Lambda\eta, \qquad \Xi_c^0 \to \Lambda\eta'$$

The spin of the ds system in the baryons Ξ_c^0 and $\Xi_c^{0\prime}$ can take on values of either 0 or 1. To simplify our analysis, we use $\Xi_c^0/\Lambda/\Sigma^0$ to refer to the baryons with a spin-0 ds system, and $\Xi_c^{\prime 0}$ to denote the baryons with a spin-1 ds system. In this study, we solely focused on the decay of Ξ_c^0 and do not consider other decay processes of $\Xi_c^{0\prime}$.

The remaining sections of this paper are organized as follows. In Sec. II, we present the theoretical framework in detail. After outlining the parametrization of the form factors for spin-1/2 to spin-1/2 processes, we provide an explicit calculation of these form factors using the light-front approach. In Sec. III, we present our numerical results for the form factors and provide a phenomenological analysis that includes decay widths and branching ratios. Finally, we conclude our work with a brief summary in the last section.

II. THEORETICAL FRAMEWORK

The nonleptonic decays under consideration are induced by the c quark transitioning to either $u\bar{d}d$ or $u\bar{s}s$. The corresponding Feynman diagram for these processes is depicted in Fig. 1.

The effective Hamiltonians for $c \to u\bar{d}d$ and $c \to u\bar{s}s$ are given as

$$\mathcal{H}(c \to u\bar{q}q) = \frac{G_F}{\sqrt{2}} V_{cq}V_{uq}^* \times \{C_1[\bar{u}_\alpha\gamma_\mu(1-\gamma_5)q_\beta][\bar{q}_\beta\gamma^\mu(1-\gamma_5)c_\alpha] + C_2[\bar{u}_\alpha\gamma_\mu(1-\gamma_5)q_\alpha][\bar{q}_\beta\gamma^\mu(1-\gamma_5)c_\beta]\}, \quad (1)$$

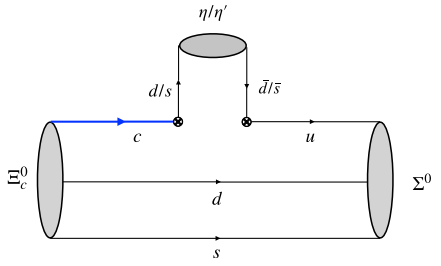

FIG. 1. The Feynman diagrams for nonleptonic decays of the heavy decay baryons we investigate.

with $q = d/s$. Utilizing the factorization ansatz, we can write down the nonleptonic decay amplitudes as

$$i\mathcal{M}(\Xi_c^0 \to \Sigma^0\eta_d) = \frac{G_F}{\sqrt{2}} V_{cd}V_{ud}^* a_2 \langle\eta(P_\eta)|\bar{d}\gamma^\mu(1-\gamma_5)d|0\rangle \times \langle\mathcal{B}_{uds}(P', S_z')|\bar{u}\gamma_\mu(1-\gamma_5)c|\Xi_c^0(P, S_z)\rangle, \quad (2)$$

$$i\mathcal{M}(\Xi_c^0 \to \Sigma^0\eta_s) = \frac{G_F}{\sqrt{2}} V_{cs}V_{us}^* a_2 \langle\eta(P_\eta)|\bar{s}\gamma^\mu(1-\gamma_5)s|0\rangle \times \langle\mathcal{B}_{uds}(P', S_z')|\bar{u}\gamma_\mu(1-\gamma_5)c|\Xi_c^0(P, S_z)\rangle, \quad (3)$$

with $a_2 = C_1 + C_2/N_c$. The C_i are Wilson coefficients at m_c scale whose values can be taken from Ref. [54]: $C_1 = -0.636$, $C_2 = 1.346$. In the above, the P and P' are the momentum of the initial and the final baryons Ξ_c^0 and Σ^0 respectively.

The hadronic contributions to these processes are described by the hadron matrix elements, which can be characterized by the form factors. In the case of spin-1/2 to spin-1/2 processes, the form factors are defined as:

$$\begin{aligned}
&\left\langle \Sigma^0\left(P', S' = \frac{1}{2}, S_z'\right)|\bar{u}\gamma_\mu(1-\gamma_5)c|\Xi_c^0\left(P, S = \frac{1}{2}, S_z\right)\right\rangle \\
&= \bar{u}(P', S_z')\left[\frac{M\gamma_\mu}{\bar{M}}f_1(q^2) + \frac{P_\mu}{\bar{M}}f_2(q^2) + \frac{P_\mu'}{\bar{M}}f_3(q^2)\right]u(P, S_z) \\
&\quad - \bar{u}(P', S_z')\left[\frac{M\gamma_\mu}{\bar{M}}g_1(q^2) + \frac{P_\mu}{\bar{M}}g_2(q^2) + \frac{P_\mu'}{\bar{M}}g_3(q^2)\right]\gamma_5 u(P, S_z), \quad (4)
\end{aligned}$$

where $\bar{M} = M - M'$.

A. Light-front quark model

The quark-diquark approximation allows us to treat baryonic systems in a manner similar to mesonic systems. In weak transitions, the two spectator quarks behave as antiquarks. This approximation has been widely employed in the study of heavy baryon decays. [55–59]. A recent study [60] explored the three-body vertex function within the light front quark model. By examining the $\Lambda_b \to \Lambda_c$ and $\Sigma_b \to \Sigma_c$ transitions, the authors found that the three-body vertex function yields results consistent with the diquark picture. This validates the use of the diquark approximation from a certain perspective.

The four-vector in the light front frame is typically represented as $v^\mu = (v^+, v^-, v_\perp)$, where $v^\pm = v^0 \pm v^3$. Within the light front quark model, a baryonic state can be described by an internal quark and diquark. The hadron state can then be expanded in terms of momentum space

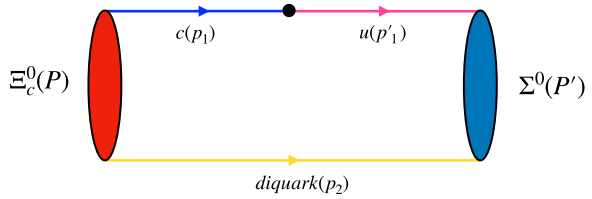

FIG. 2. The diquark approximation for the baryonic transition.

and flavor-spin functions. For a spin-1/2 baryon state, this expansion takes the form:

$$|\Xi_c^0(P,S,S_z)\rangle = \int \{d^3p_1\}\{d^3p_2\}2(2\pi)^3\delta^3(\tilde{P}-\tilde{p}_1-\tilde{p}_2) \times \sum_{\lambda_1,\lambda_2}\Psi^{SS_z}(\tilde{p}_1,\tilde{p}_2,\lambda_1,\lambda_2)| \times c(p_1,\lambda_1)(\mathrm{di})(p_2,\lambda_2)\rangle, \quad (5)$$

In the above equation, the term "(di)" corresponds to the diquark shown in Fig. 2, and their helicities are denoted by λ_1 and λ_2. The momenta of the baryon, quark, and diquark are represented by P, p_1, and p_2, respectively. The momenta $\tilde{P}$, $\tilde{p}_1$, and $\tilde{p}_2$ are three-dimensional momenta, denoted by $\tilde{p} = (p^+, p_\perp)$. It is important to note that the on-shell momentum has only three degrees of freedom despite having four components. As a result, the minus component of the momentum is fixed by the relation $p^- = (m^2 + p_\perp^2)/p^+$.

The wave function Ψ in Eq. (5) can be expressed as a combination of spin and momentum space functions. Specifically, it can be decomposed as:

$$\Psi^{SS_z}(\tilde{p}_1,\tilde{p}_2,\lambda_1,\lambda_2) = \frac{1}{\sqrt{2(p_1\cdot\bar{P}+m_1M_0)}} \times \bar{u}(p_1,\lambda_1)\Gamma_{S(A)}u(\bar{P},S_z)\phi(x,k_\perp). \quad (6)$$

As previously mentioned, the diquark can exist in either a spin-0 scalar or spin-1 axial-vector state. In the case of a scalar diquark, the interaction vertex Γ is given by $\Gamma_S = 1$. On the other hand, for a spin-1/2 baryon with an axial-vector diquark, the corresponding interaction vertex takes the form:

$$\Gamma_A = \frac{\gamma_5}{\sqrt{3}}\left(\not{\epsilon}^*(p_2,\lambda_2) - \frac{M_0+m_1+m_2}{\bar{P}\cdot p_2+m_2M_0}\epsilon^*(p_2,\lambda_2)\cdot\bar{P}\right). \quad (7)$$

In the above equation, m_1 and m_2 represent the masses of the quark and spectator diquark, respectively. The quantity $\bar{P}$ is the on-shell momentum of the light quark q and diquark, and satisfies the conditions $\bar{P} = p_1 + p_2$ and $\bar{P}^2 = M_0^2$. Here, M_0 represents the invariant mass of $\bar{P}$, which differs from the baryon mass M due to the fact that the quark, diquark, and baryon cannot all be on their respective mass shells simultaneously. The momentum P and mass M of the baryon, however, must satisfy the physical mass-shell condition, $M^2 = P^2$. It is important to note that the momentum $\bar{P}$ is not equal to P.

In the equation (6), ϕ represents a Gaussian-type function constructed as:

$$\phi = 4\left(\frac{\pi}{\beta^2}\right)^{3/4}\sqrt{\frac{e_1e_2}{x_1x_2M_0}}\exp\left(\frac{-\vec{k}^2}{2\beta^2}\right), \quad (8)$$

Here, e_1 and e_2 represent the energies of the quark q and diquark in the rest frame of $\bar{P}$. The variables x_1 and x_2 correspond to the light-front momentum fractions and satisfy the conditions $0 < x_2 < 1$ and $x_1 + x_2 = 1$. The internal motion of the constituent quarks is described by the internal momentum $\vec{k}$. The internal light front momentum and related dynamic relationships are given as:

$$\begin{aligned} k_i &= (k_i^-, k_i^+, k_{i\perp}) = (e_i - k_{iz}, e_i + k_{iz}, k_{i\perp}) \\ &= \left(\frac{m_i^2+k_{i\perp}^2}{x_iM_0}, x_iM_0, k_{i\perp}\right), \\ p_1^+ &= x_1\bar{P}^+, \qquad p_2^+ = x_2\bar{P}^+, \qquad p_{1\perp} = x_1\bar{P}_\perp + k_{1\perp}, \\ p_{2\perp} &= x_2\bar{P}_\perp + k_{2\perp}, \qquad k_\perp = -k_{1\perp} = k_{2\perp}. \end{aligned} \quad (9)$$

The $\vec{k}$ in the Eq. (8) is the internal three-momentum vector of diquark presented as $\vec{k} = (k_{2\perp}, k_{2z}) = (k_\perp, k_z)$. The parameter β appearing in Eq. (8) represents the momentum distribution between the constituent quarks. By using the definition of the internal three-momentum vector, we can express the invariant mass squared M_0^2 as a function of the variables $(x_i, k_{i\perp})$,

$$M_0^2 = \frac{k_{1\perp}^2+m_1^2}{x_1} + \frac{k_{2\perp}^2+m_2^2}{x_2}. \quad (10)$$

The energy e_i and k_z can also be expressed in terms of the internal variables $(x_i, k_{i\perp})$ as follows:

$$\begin{aligned} e_i &= \frac{x_iM_0}{2} + \frac{m_i^2+k_{i\perp}^2}{2x_iM_0} = \sqrt{m_i^2+k_{i\perp}^2+k_{iz}^2}, \\ k_{iz} &= \frac{x_iM_0}{2} - \frac{m_i^2+k_{i\perp}^2}{2x_iM_0}. \end{aligned} \quad (11)$$

In what follows, we adopt the notation $x = x_2$ and $x_1 = 1 - x$.

B. Form factors

The hadron matrix element for the spin-1/2 to spin-1/2 processes can be expressed as:

$$\left\langle \Sigma^0\left(P',\frac{1}{2},S'_z\right)|\bar{u}\gamma^\mu(1-\gamma_5)c|\Xi_c^0\left(P,\frac{1}{2},S_z\right)\right\rangle$$
$$=\int\{d^3p_2\}\frac{\phi'(x',k'_\perp)\phi(x,k_\perp)}{2\sqrt{p_1^+p_1'^+}(p_1\cdot\bar{P}+m_1M_0)(p'_1\cdot\bar{P}'+m'_1M'_0)}$$
$$\times\sum_{\lambda_2}\bar{u}(\bar{P}',S'_z)[\bar{\Gamma}'(\not{p}'_1+m'_1)\gamma^\mu(1-\gamma_5)(\not{p}_1+m_1)\Gamma]$$
$$\times u(\bar{P},S_z). \tag{12}$$

where

$$m_1=m_c,\quad m'_1=m_u,\quad m_2=m_{(di)},\quad \bar{P}=p_1+p_2,$$
$$\bar{P}'=p'_1+p_2,\quad M_0^2=\bar{P}^2,\quad M_0'^2=\bar{P}'^2. \tag{13}$$

The momenta of the c quark in the initial baryon and u quark in the final baryon are denoted by p_1 and p'_1, respectively. The variable p_2 represents the momentum of the spectator diquark. The quantities P and P' denote the four-momenta of the initial and final baryon states, respectively, while M and M' correspond to their physical masses.

It is noted that one can also define M_0 and M'_0 for the initial and final baryon states, respectively, such that $\bar{P}^{(\prime)2}=M_0^{(\prime)2}$. The quantity $\bar{\Gamma}$ appearing in Eq. (12) is defined as:

$$\Gamma_S=\bar{\Gamma}'_S=1,$$
$$\bar{\Gamma}'_A=\frac{1}{\sqrt{3}}\left(-\not{\epsilon}(p_2,\lambda_2)+\frac{M'_0+m'_1+m_2}{\bar{P}'\cdot p_2+m_2M'_0}\epsilon(p_2,\lambda_2)\cdot\bar{P}'\right)\gamma_5. \tag{14}$$

By comparing the LFQM results for the hadron matrix element with Eq. (4), we can extract the form factors by solving the following equations:

$$\mathrm{Tr}\left\{(\not{P}'+M')\left[\frac{M\gamma_\mu}{\bar{M}}f_1^{\frac{1}{2}\to\frac{1}{2}}(q^2)+\frac{P_\mu}{\bar{M}}f_2^{\frac{1}{2}\to\frac{1}{2}}(q^2)+\frac{P'_\mu}{\bar{M}}f_3^{\frac{1}{2}\to\frac{1}{2}}(q^2)\right](\not{P}+M)\{\Gamma_i\}_\mu\right\}=H_i^{\frac{1}{2}},$$
$$\mathrm{Tr}\left\{(\not{P}'+M')\left[\frac{M\gamma_\mu}{\bar{M}}g_1^{\frac{1}{2}\to\frac{1}{2}}(q^2)+\frac{P_\mu}{\bar{M}}g_2^{\frac{1}{2}\to\frac{1}{2}}(q^2)+\frac{P'_\mu}{\bar{M}}g_3^{\frac{1}{2}\to\frac{1}{2}}(q^2)\right]\gamma_5(\not{P}+M)\{\Gamma_{5i}\}_\mu\right\}=K_i^{\frac{1}{2}},\qquad i=1,2,3 \tag{15}$$

where $H_i^{\frac{1}{2}}$, $K_i^{\frac{1}{2}}$ are defined as

$$H_i^{\frac{1}{2}}=\int\frac{dxd^2k_\perp}{2(2\pi)^3}\frac{\phi'(x',k'_\perp)\phi(x,k_\perp)}{2\sqrt{x'_1x_1}(p'_1\cdot\bar{P}'+m'_1M'_0)(p_1\cdot\bar{P}+m_1M_0)}$$
$$\times\mathrm{Tr}\{(\bar{\not{P}}'+M'_0)\Gamma'_{S(A)}(\not{p}'_1+m'_1)\gamma_\mu(\not{p}_1+m_1)\Gamma_{S(A)}(\bar{\not{P}}+M_0)\{\Gamma_i\}_\mu\}$$
$$K_i^{\frac{1}{2}}=\int\frac{dxd^2k_\perp}{2(2\pi)^3}\frac{\phi'(x',k'_\perp)\phi(x,k_\perp)}{2\sqrt{x'_1x_1}(p'_1\cdot\bar{P}'+m'_1M'_0)(p_1\cdot\bar{P}+m_1M_0)}$$
$$\times\mathrm{Tr}\{(\bar{\not{P}}'+M'_0)\Gamma'_{S(A)}(\not{p}'_1+m'_1)\gamma_\mu\gamma_5(\not{p}_1+m_1)\Gamma_{S(A)}(\bar{\not{P}}+M_0)\{\Gamma_{5i}\}_\mu\}, \tag{16}$$

The different Dirac structures Γ_i and Γ_{5i} are

$$\{\Gamma_i\}_\mu=\{\gamma_\mu,P_\mu,P'_\mu\},$$
$$\{\Gamma_{5i}\}_\mu=\{\gamma_\mu\gamma_5,P_\mu\gamma_5,P'_\mu\gamma_5\}, \tag{17}$$

Then the form factors are solved as

$$f_1^{\frac{1}{2}\to\frac{1}{2}}=-\frac{\bar{M}(s_+H_1^{\frac{1}{2}}-2M'H_2^{\frac{1}{2}}-2MH_3^{\frac{1}{2}})}{4Ms_-s_+},$$
$$f_2^{\frac{1}{2}\to\frac{1}{2}}=\frac{\bar{M}(M's_+H_1^{\frac{1}{2}}-6M'^2H_2^{\frac{1}{2}}+2(s_-+MM')H_3^{\frac{1}{2}})}{2s_-s_+^2},$$
$$f_3^{\frac{1}{2}\to\frac{1}{2}}=\frac{\bar{M}(Ms_+H_1^{\frac{1}{2}}+2(s_-+MM')H_2^{\frac{1}{2}}-6M^2H_3^{\frac{1}{2}})}{2s_-s_+^2}. \tag{18}$$

Here, $s_\pm=(M\pm M')^2-q^2$, and the form factors $g_i^{\frac{1}{2}\to\frac{1}{2}}$ can be obtained by applying the following transformation:

$$M'\to-M',\quad \bar{M}\to\bar{M},\quad H_j\to K_j,\quad i=1$$
$$M'\to-M',\quad \bar{M}\to\bar{M},\quad H_j\to-K_j,\quad i=2,3. \tag{19}$$

As the diquark can be either scalar or axial-vector, the physical baryon state is a combination of the baryon state with a scalar diquark and a state with an axial-vector diquark in LFQM. Therefore, the physical form factor can also be expressed as follows:

$$[\mathrm{formfactor}]^{\mathrm{physical}}=c_S\times[\mathrm{formfactor}]_S+c_A\times[\mathrm{formfactor}]_A. \tag{20}$$

TABLE I. The spin factors for the baryon Ξ_c^0 decay induced by $c \to u$.

Channel	c_S	c_A
$\Xi_c^0 \to \Sigma^0$	$\frac{\sqrt{3}}{2}$	0
$\Xi_c^0 \to \Lambda$	$\frac{1}{2}$	0

The coefficients c_S and c_A are flavor-spin factors that can be determined by the flavor-spin wave function of baryons in the diquark basis. The flavor-spin wave functions for spin-1/2 baryons are given by:

$$\begin{aligned}\Sigma^0 &= \frac{\sqrt{3}}{2}u[ds]_S - \frac{1}{2}u[ds]_A \\ \Lambda &= \frac{1}{2}u[ds]_S + \frac{\sqrt{3}}{2}u[ds]_A \\ \Xi_c^0 &= c[ds]_S. \end{aligned} \tag{21}$$

The flavor wave functions of the diquark basis are given by:

$$\begin{aligned}[q_1q_2]_A &= \frac{1}{\sqrt{2}}(q_1q_2 + q_2q_1), \\ [q_1q_2]_S &= \frac{1}{\sqrt{2}}(q_1q_2 - q_2q_1). \end{aligned} \tag{22}$$

Therefore, the overlapping factors can be calculated and the results are presented in Table I.

TABLE II. baryon masses [64,65] and other input parameters [66,67].

Baryon	Ξ_c^0	Σ^0	Λ	η	η'
Mass (GeV)	2.470	1.193	1.116	0.548	0.958
Lifetime (fs)	151.9				
$\beta_{[ds]c} = 0.58$			$\beta_{[ds]u} = 0.41$		

III. NUMERICAL RESULTS

After deriving the analytic expression in the LFQM, we present the corresponding numerical results. For the calculation, we use the quark masses from Refs. [61–63]

$$\begin{aligned} &m_u = m_d = 0.25\ \text{GeV}, \qquad m_s = 0.37\ \text{GeV}, \\ &m_c = 1.4\ \text{GeV}. \end{aligned} \tag{23}$$

The masses of the diquarks can be approximated as

$$m_{[ds]} = m_d + m_s. \tag{24}$$

The masses of the baryons, their lifetimes, and the input parameter $\beta_{[ds]q}$ are presented in Table II.

A. Form factors

To analyze the q^2 dependence of the form factors in Eq. (4), we adopt the double-pole model parametrization scheme as follows:

$$F(q^2) = \frac{F(0)}{1 - \frac{q^2}{m_{\text{fit}}^2} + \delta\left(\frac{q^2}{m_{\text{fit}}^2}\right)^2}, \tag{25}$$

TABLE III. Numerical results for the form factors of spin-1/2 to spin-1/2 $\Xi_c^0 \to \Sigma(\Lambda)$ transitions. The F(0) indicates the form factors when $q^2 = 0$. Results for the parameters δ and m_{fit} are obtained by fitting the form factors with the double-pole model as in Eq. (25). The α_0 and α_1 are the parameters in the BCL model in Eq. (26). For the form factors $F(0)$ with $q^2 = 0$, we estimated their uncertainties caused by the parameters in LFQM, namely, $\beta_{c[ds]}$, $\beta_{u[ds]}$, and m_{di}, which are varied by 10%.

		Pole model			BCL model	
Channel	Form factor	F(0)	m_{fit}	δ	α_0	α_1
$\Xi_c^0 \to \Sigma^0$	f_1	$0.5988 \pm 0.0765 \pm 0.0500 \pm 0.0407$	1.98	0.40	0.5827	0.9969
	f_2	$0.1288 \pm 0.0222 \pm 0.0477 \pm 0.0100$	0.78	0.50	0.2784	−9.2418
	f_3	$-0.5504 \pm 0.1055 \pm 0.0934 \pm 0.0513$	1.05	0.23	−0.8453	18.2072
	g_1	$0.3838 \pm 0.0133 \pm 0.0384 \pm 0.0168$	2.46	1.15	0.3432	2.5073
	g_2	$-0.4279 \pm 0.1518 \pm 0.1303 \pm 0.0593$	2.64	20.5	−0.3765	−3.1717
	g_3	$1.1520 \pm 0.1626 \pm 0.2791 \pm 0.1190$	1.30	0.60	1.4584	−18.9181
$\Xi_c^0 \to \Lambda$	f_1	$0.3382 \pm 0.0432 \pm 0.0290 \pm 0.0229$	2.12	0.70	0.3167	1.1188
	f_2	$0.1188 \pm 0.0170 \pm 0.0318 \pm 0.0081$	0.90	0.42	0.2283	−5.6985
	f_3	$-0.3471 \pm 0.0640 \pm 0.0583 \pm 0.0314$	1.06	0.26	−0.5498	10.5412
	g_1	$0.2536 \pm 0.0093 \pm 0.0245 \pm 0.0108$	2.32	0.64	0.2284	1.3106
	g_2	$-0.2977 \pm 0.0751 \pm 0.0694 \pm 0.0319$	1.66	1.48	−0.3204	1.1828
	g_3	$0.8241 \pm 0.0758 \pm 0.1591 \pm 0.0685$	1.21	0.37	1.1416	−16.5172

where $F(0)$ is the numerical results of form factor at $q^2 = 0$. And we take $\{-0.000, -0.001, -0.005, -0.007, -0.01, -0.015\}$ for q^2 and fit the two parameters $m_{\rm fit}$ and δ. Table III presents the numerical results for the form factors and fitting parameters obtained using the double-pole model which parametrizes the q^2 dependence of the form factors. Additionally, for extrapolating the form factors to the full q^2 region, we use the Bourrely-Caprini-Lellouch (BCL) parametrization [68–71] in which the form factors are expanded in powers of a conformal mapping variable. The BCL parametrization is shown as

$$\begin{aligned} f(q^2) &= \frac{1}{1-q^2/m_R^2}\sum_{k=0}^{k_{\rm max}} \alpha_k z^k(q^2,t_0), \\ z(q^2,t_0) &= \frac{\sqrt{t_+ - q^2} - \sqrt{t_+ - t_0}}{\sqrt{t_+ - q^2} + \sqrt{t_+ - t_0}}, \\ t_0 &= t_+\left(1 - \sqrt{1 - \frac{t_-}{t_+}}\right), \\ t_\pm &= (m_{\mathcal{B}_b} \pm m_{\mathcal{B}_c})^2. \end{aligned} \tag{26}$$

The m_R are the masses of the low-lying D resonance.

To analyze the q^2 dependence of the form factors, we also plot the results of the form factors as functions of q^2 in Fig. 3. From Fig. 3, one can see that the fit results with two different models are broadly consistent with each other. However, the q^2-dependent form factor g_2 exhibits a large discrepancy with $q^2 \sim (m_{\mathcal{B}_c} - m_{\mathcal{B}_u})^2$ for the two models. In the analysis presented in Ref. [59], the form factor has a pole structure corresponding to the specific current. In our work, the pole mass $m_{\rm pole}$ should be set to $m_{\rm pole} = m_D$, which is consistent with the BCL model in Eq. (26). However, the fit result of g_2 with the pole model is some different from our conclusion, especially for the $\Xi_c^0 \to \Sigma^0$ process. Therefore, it is likely that the BCL model describes the q^2 dependence of the form factor better.

B. Nonleptonic decays

Expressing the physical states η and η' in the quark flavor basis, we have:

$$\begin{pmatrix} |\eta\rangle \\ |\eta'\rangle \end{pmatrix} = \begin{pmatrix} \cos\phi & -\sin\phi \\ \sin\phi & \cos\phi \end{pmatrix} \begin{pmatrix} |\eta_q\rangle \\ |\eta_s\rangle \end{pmatrix} \tag{27}$$

where ϕ denotes the mixing angle. Nonleptonic decay with $\eta^{(\prime)}$ emission can be estimated with the helicity amplitude method. In Eq. (3), the local matrix element $\langle\eta^{(\prime)}(P)|\bar{s}\gamma^\mu(1-\gamma_5)s|0\rangle$ and $\langle\eta^{(\prime)}(P)|\bar{d}\gamma^\mu(1-\gamma_5)d|0\rangle$ can be expressed by the decay constant $f^s_{\eta^{(\prime)}}$ and $f^d_{\eta^{(\prime)}}$ as [72–74]

$$\begin{aligned} \langle 0|\bar{q}\gamma^\mu(1-\gamma_5)q|\eta_q(P)\rangle &= \frac{i}{\sqrt{2}} f_q P^\mu, \\ \langle 0|\bar{s}\gamma^\mu(1-\gamma_5)s|\eta_s(P)\rangle &= i f_s P^\mu \end{aligned} \tag{28}$$

where all the other parameters are listed below

$$\begin{aligned} &m_\eta = 0.548\ \text{GeV}, \qquad m_{\eta'} = 0.958\ \text{GeV}, \\ &f_q = 1.07 f_\pi, \qquad f_s = 1.34 f_\pi, \\ &f_\pi = 0.130\ \text{GeV}, \qquad \phi = 39.3^\circ, \end{aligned} \tag{29}$$

Then the amplitude of nonleptonic decays becomes

$$\begin{aligned} i\mathcal{M}(\Xi_c^0 \to \Sigma^0\eta) &= \frac{iG_F}{\sqrt{2}} P_\eta^\mu \left(\frac{\cos\phi}{\sqrt{2}} V_{cd}V_{ud}^* f_q - \sin\phi V_{cs}V_{us}^* f_s\right) \\ &\quad a_2\langle\Sigma^0(P', S_z')|\bar{u}\gamma_\mu(1-\gamma_5)c|\Xi_c^0(P, S_z)\rangle \\ i\mathcal{M}(\Xi_c^0 \to \Sigma^0\eta') &= \frac{iG_F}{\sqrt{2}} P_{\eta'}^\mu \left(\frac{\sin\phi}{\sqrt{2}} V_{cd}V_{ud}^* f_q + \cos\phi V_{cs}V_{us}^* f_s\right) \\ &\quad a_2\langle\Sigma^0(P', S_z')|\bar{u}\gamma_\mu(1-\gamma_5)c|\Xi_c^0(P, S_z)\rangle \end{aligned} \tag{30}$$

The helicity amplitudes in the nonleptonic decay processes are defined as

$$\begin{aligned} HV^S_{\lambda,\lambda'} &= \langle\Sigma^0(P',\lambda')|\bar{u}\not{P}_{\eta^{(\prime)}}c|\Xi_c^0(P,\lambda)\rangle, \\ HA^S_{\lambda,\lambda'} &= \langle\Sigma^0(P',\lambda')|\bar{u}\not{P}_{\eta^{(\prime)}}\gamma_5 c|\Xi_c^0(P,\lambda)\rangle. \end{aligned} \tag{31}$$

With the help of helicity amplitude, the total decay width of the spin-1/2 to spin-1/2 processes can be expressed as

$$\begin{aligned} \Gamma^{\frac{1}{2}\to\frac{1}{2}} &= \mathcal{P}_{\eta^{(\prime)}} \frac{\sqrt{s_+ s_-}}{32\pi M^3}\left(|H^{\frac{1}{2}}_{\frac{1}{2},-\frac{1}{2}}|^2 + |H^{\frac{1}{2}}_{-\frac{1}{2},\frac{1}{2}}|^2\right), \\ \mathcal{P}_\eta &= \frac{G_F^2}{2}\left(\left(\frac{\cos\phi}{\sqrt{2}} V_{cd}V_{ud}^* f_q\right)^2 + (\sin\phi V_{cs}V_{us}^* f_s)^2\right) a_2^2, \\ \mathcal{P}_{\eta'} &= \frac{G_F^2}{2}\left(\left(\frac{\sin\phi}{\sqrt{2}} V_{cd}V_{ud}^* f_q\right)^2 + (\cos\phi V_{cs}V_{us}^* f_s)^2\right) a_2^2, \end{aligned} \tag{32}$$

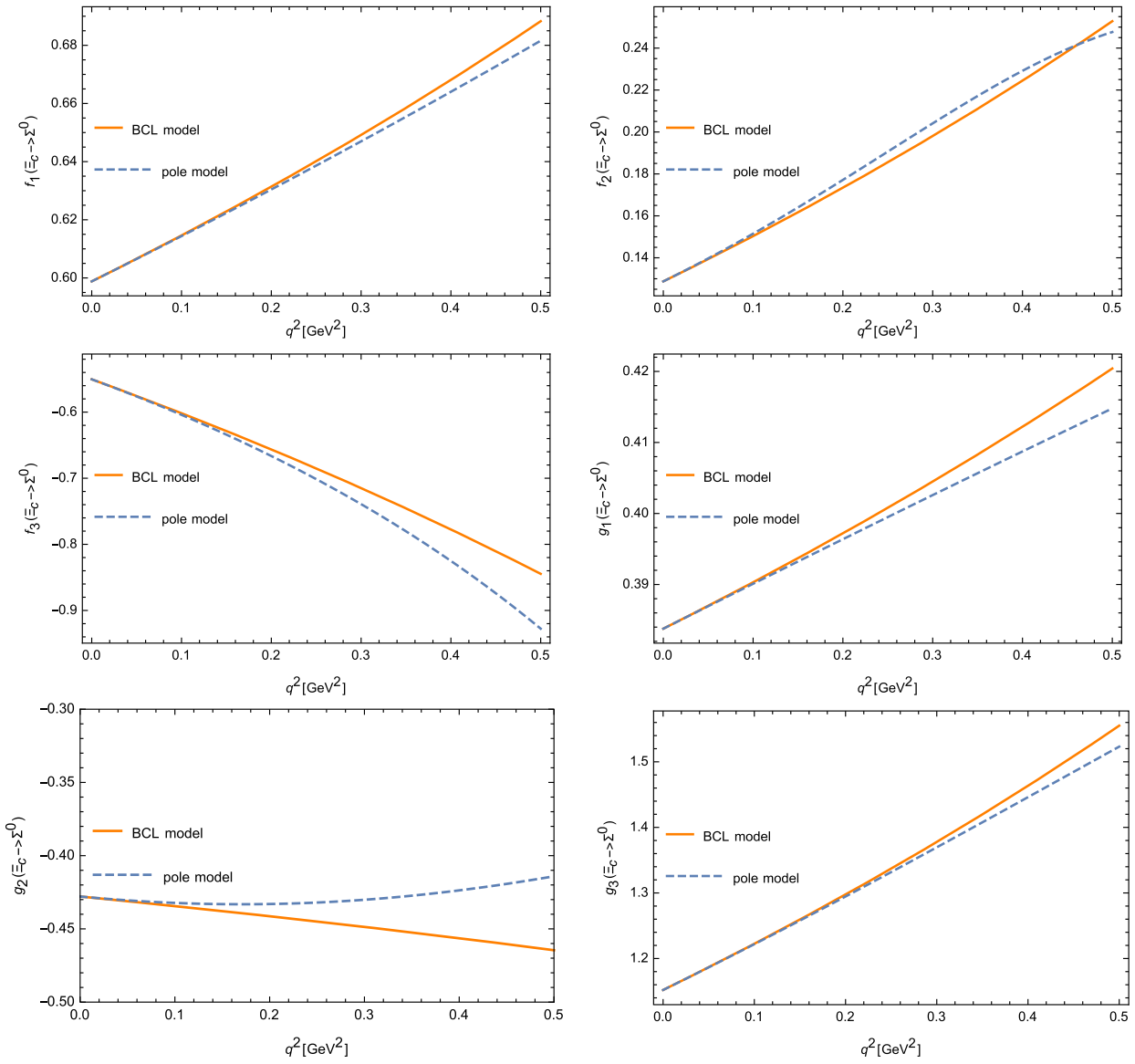

FIG. 3. The q^2 dependence form factors of $\Xi_c^0 \to \Sigma^0$ process with BCL model (Orange line) and pole model (blue line).

where $H^S_{\lambda,\lambda'} = HV^S_{\lambda,\lambda'} - HA^S_{\lambda,\lambda'}$. The expressions of the nonleptonic helicity amplitudes are shown in the Appendix. Although we have not accounted for the nonfactorizable contributions, we can estimate their impact by varying the value of N_c. A method outlined in Ref. [47] suggests that adjusting the value of N_c in the Wilson coefficient $a_2 = C_1 + C_2/N_c$ can help estimate these contributions in B decays. Since there are no experimental results for these two specific processes at present, we can use a similar process, namely $\Xi_c^0 \to \Lambda\phi$ [75], which does have experimental data available, to determine the value of N_c. To determine the appropriate value for N_c, we examine the corresponding Feynman diagram, shown in Fig. 4.

So the way we compute the branching ratio for this process. we vary the value of N_c and determine that the

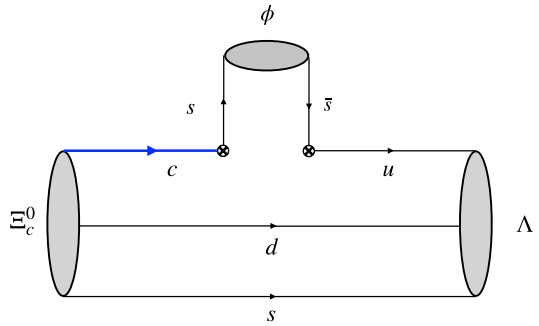

FIG. 4. The Feynman diagrams for nonleptonic decays of the decay $\Xi_c^0 \to \Lambda\phi$ we investigate.

TABLE IV. Numerical results of decay width and branching fraction in heavy baryon nonleptonic decays using BCL model $f(q^2)$ at $N_c = 5.4 \pm 1.2$. We have assessed the uncertainties arising from variations in N_c and the parameters within LFQM, namely, $\beta_{c[ds]}$, $\beta_{u[ds]}$, and m_{di}, each of which was subject to a 10% variation.

Channel	$\Gamma(\times 10^{-16}$ GeV)	Br(10^{-4})
$\Xi_c^0 \to \Sigma^0\eta$	$4.85 \pm 1.62 \pm 0.51 \pm 0.39 \pm 0.34$	$1.12 \pm 0.38 \pm 0.12 \pm 0.09 \pm 0.08$
$\Xi_c^0 \to \Sigma^0\eta'$	$6.64 \pm 2.22 \pm 0.92 \pm 0.76 \pm 0.85$	$1.53 \pm 0.51 \pm 0.21 \pm 0.18 \pm 0.19$

branching ratio matches the experimental result of $4.9 \pm 1.5 \times 10^{-4}$. Specifically, we find that the branching ratio equals the experimental value when $N_c = 5.4 \pm 1.2$. Using the formulas above and choosing $N_c = 5.4 \pm 1.2$, we give numerical results of hadron nonleptonic two-body decays in Table IV.

Using the formulas above, we give numerical results of the nonleptonic two-body decay processes $\Xi_c^0 \to \Sigma^0\eta^{(\prime)}$ in Table V and $\Xi_c^0 \to \Lambda\eta^{(\prime)}$ in Table IV.

There are other procedures used for similar processes that suggest different values for N_c, for example, Ref. [75] suggests that N_c may be around 7 according to the process $\Lambda^+ \to p\phi$. We can roughly estimate the nonfactorization effect by varying the N_c. This strategy is used in Ref. [12], it has been suggested that the nonfactorizable contributions in B decays can be estimated through a variation of N_c in Wilson coefficient a_1 or a_2. In accordance with our selection criteria and the criteria adopted in reference [75], the chosen range for our parameter N_c is as follows $3, 5.4, \infty$. The effects are estimated in Table VI. The results show that for this kind of processes $\Xi_c^0 \to \Sigma^0\eta/\eta'$ or $\Xi_c^0 \to \Lambda^0\eta/\eta'$, the decay width and branching fraction varies somewhat with different N_c. In Table VI, we also show the results of the branching ratios obtained by global fit and MIT-bag in Refs. [28,29]. The outcomes of our results align closely with those of reference [28] within the margin of error. However, it is noteworthy that the central value of the process $\Xi_c^0 \to \Lambda\eta'$ exhibits a specific deviation. When considering the error, the two results also remain consistent within the margin of error. In comparison to Ref. [29], it appears that the central values of our results exhibit an order of magnitude difference (it seems the error associated with Ref. [29] is not presented). Reference [28] study a series of decays of the charmed baryon state based on the SU(3) flavor symmetry. In Ref. [29], both factorizable and nonfactorizable contributions are considered in the topologic diagram approach. To explore less model-dependent observables, we can utilize the ratios of branching ratios for certain decay channels as a means to study the variations in decay widths resulting from different values of N_c. Therefore one can define the value $\mathcal{R}_{\Sigma^0(\Lambda)}$ as

$$\mathcal{R}_{\Sigma^0} = \frac{\Gamma(\Xi_c^0 \to \Sigma^0\eta)}{\Gamma(\Xi_c^0 \to \Sigma^0\eta')},$$
$$\mathcal{R}_{\Lambda} = \frac{\Gamma(\Xi_c^0 \to \Lambda\eta)}{\Gamma(\Xi_c^0 \to \Lambda\eta')}. \tag{33}$$

The values of these ratios are shown in Table VI. This ratio is a quantity independent of the parameter N_c, indicating reduced model dependence in the observables. This enhanced predictability makes it a valuable candidate for experimental testing.

Before closing this section we wish to point out that our analysis did not take the imaginary part of the decay amplitudes into account. In principle, the imaginary part could be important especially in the study of CP violation, and may arise from two different sources: the perturbative contributions such as quark loops; or the long-distance contributions from such as final state interactions (see Refs. [76,77] for example). Usually in QCD approach like QCD factorization [78], quark loops can be expressed as a vertex correction to the effective Wilson coefficients. Although it is unlikely to attribute these corrections into the effective color number, it is likely that varying the N_c may partially reflect the size of such corrections. The generalized factorization approach before the QCD factorization has used this method to estimate the uncertainties [12]. For the long-distance contributions, a systematic analysis is not available for charmed baryon decays especially in the absence of a collection of all available effective couplings at the hadron level. We hope this can be conducted in an improved analysis in the future.

TABLE V. Numerical results of decay width and branching fraction in heavy baryon nonleptonic decays using BCL model $f(q^2)$ at $N_c = 5.4 \pm 1.2$. We have assessed the uncertainties arising from variations in N_c and the parameters within LFQM, namely, $\beta_{c[ds]}$, $\beta_{u[ds]}$, and m_{di}, each of which was subject to a 10% variation.

Channel	$\Gamma(\times 10^{-16}$ GeV)	Br(10^{-4})
$\Xi_c^0 \to \Lambda\eta$	$1.70 \pm 0.57 \pm 0.18 \pm 0.14 \pm 0.13$	$0.39 \pm 0.13 \pm 0.04 \pm 0.03 \pm 0.03$
$\Xi_c^0 \to \Lambda\eta'$	$2.53 \pm 0.85 \pm 0.35 \pm 0.27 \pm 0.31$	$0.58 \pm 0.19 \pm 0.08 \pm 0.06 \pm 0.07$

TABLE VI. Numerical results of decay width and branching fraction in doubly heavy baryon nonleptonic decays using $f(q^2)$ when $N_c = 3, 5.4, \infty$.

		$N_c = 3$		$N_c = 5.4$		$N_c = \infty$		Reference [28]	Reference [29]
Channel	$\mathcal{R}$	$\Gamma(\times 10^{-16}$ GeV)	$\mathrm{Br}(10^{-4})$	$\Gamma(\times 10^{-16}$ GeV)	$\mathrm{Br}(10^{-4})$	$\Gamma(\times 10^{-16}$ GeV)	$\mathrm{Br}(10^{-4})$	$\mathrm{Br}(10^{-4})$	$\mathrm{Br}(10^{-4})$
$\Xi_c^0 \to \Sigma^0\eta$	0.73	1.14	0.26	4.85	1.12	13.12	3.02	$3.6^{+1.0}_{-0.9}$	5.0
$\Xi_c^0 \to \Sigma^0\eta'$		1.56	0.36	6.64	1.53	17.96	4.13	$1.7^{+3.0}_{-1.5}$	
$\Xi_c^0 \to \Lambda\eta$	0.68	0.40	0.09	1.70	0.39	4.61	1.06	$1.6^{+1.2}_{-0.8}$	8.1
$\Xi_c^0 \to \Lambda\eta'$		0.59	0.14	2.53	0.58	6.83	1.57	$9.4^{+11.6}_{-6.8}$	

IV. SUMMARY

The two-body hadronic decays decays of the baryons $\Xi_c^0 \to \Sigma^0\eta^{(\prime)}$ and $\Xi_c^0 \to \Lambda\eta^{(\prime)}$ are studied in this work. In this work, we employed the light-front-quark model to study nonleptonic decays of the baryons Ξ_c^0. Specifically, we utilized the diquark picture, where the two spectator heavy quarks can be approximated as a scalar or an axial-vector diquark, and treated the baryon state as a meson state. We obtained the form factors defined by the hadronic matrix element of the effective operators sandwiched between the Ξ_c^0 and the light baryon state and then used them to estimate the decay widths and branching fractions of two-body nonleptonic decays.

We have used the helicity amplitudes to obtain the phenomenological results, which include the predicted branching fractions. With the lifetime of Ξ_c^0 presented in Table II, we have calculated the branching fractions and listed them in Table IV. Lastly, we explore the dependence on N_c and introduce new observations denoted as $\mathcal{R}$, which exhibit minimal sensitivity to parameters. These quantities are less model-dependent, rendering them suitable for experimental testing. This study represents an exploratory endeavor, taking into account the nonperturbative nature of matrix elements. To delve deeper into these nonperturbative matrix elements, we also plan to employ the first-principle lattice method for conducting additional calculations. The obtained phenomenological results are helpful in the search for such types of decay processes in future experiments.

ACKNOWLEDGMENTS

We thank Zhi-Peng Xing, Prof. Wei Wang, Prof. Xiao-Gang He, Meng-Lin Du, C. W. Liu, and Zhen-Xing Zhao for their useful discussions. The research received partial funding from the National Natural Science Foundation of China (NSFC) under the Grants No. 12125503, No. U2032102, No. 12335003.

APPENDIX: HELICITY AMPLITUDE

The helicity amplitudes for the spin-1/2 to spin-1/2 nonleptonic decay processes can be expressed in terms of the form factors defined in the hadron matrix element. Here, we define $(M^2 - M'^2) \pm q^2 = \hat{M}_q^{\pm}$. The helicity amplitudes can then be written as follows:

$$
\begin{aligned}
HV^{\frac{1}{2}}_{-\frac{1}{2},\frac{1}{2}} &= \frac{-i\sqrt{s_+}m_\eta}{2\bar{M}\sqrt{q^2}}[2M\bar{M}f_1^{\frac{1}{2}\to\frac{1}{2}} + \hat{M}_q^+ f_2^{\frac{1}{2}\to\frac{1}{2}} + \hat{M}_q^- f_3^{\frac{1}{2}\to\frac{1}{2}}],\\
HV^{\frac{1}{2}}_{-\lambda,-\lambda'} &= HV^{\frac{1}{2}}_{\lambda,\lambda'},\\
HA^{\frac{1}{2}}_{-\frac{1}{2},\frac{1}{2}} &= \frac{-i\sqrt{s_-}m_\eta}{2\bar{M}\sqrt{q^2}}[2M(M+M')g_1^{\frac{1}{2}\to\frac{1}{2}}\\
&\quad - \hat{M}_q^+ g_2^{\frac{1}{2}\to\frac{1}{2}} - \hat{M}_q^- g_3^{\frac{1}{2}\to\frac{1}{2}}],
\end{aligned}
\tag{A1}
$$

$$
HA^{\frac{1}{2}}_{-\lambda,-\lambda'} = -HA^{\frac{1}{2}}_{\lambda,\lambda'}. \tag{A2}
$$

[1] M. Ablikim *et al.* (BESIII Collaboration), Phys. Lett. B **783**, 200 (2018).
[2] M. Ablikim *et al.* (BESIII Collaboration), Phys. Rev. Lett. **121**, 062003 (2018).
[3] J. Y. Lee *et al.* (Belle Collaboration), Phys. Rev. D **103**, 052005 (2021).
[4] X. R. Lyu (BESIII Collaboration), Proc. Sci. CHARM2020 (**2021**) 016.
[5] X. G. He, Y. J. Shi, and W. Wang, Eur. Phys. J. C **80**, 359 (2020).
[6] D. Wang, P. F. Guo, W. H. Long, and F. S. Yu, J. High Energy Phys. 03 (2018) 066.

[7] H. J. Zhao, Y. L. Wang, Y. K. Hsiao, and Y. Yu, J. High Energy Phys. 02 (2020) 165.
[8] C. Q. Geng, C. W. Liu, and T. H. Tsai, Phys. Lett. B **794**, 19 (2019).
[9] C. K. Chua, Phys. Rev. D **97**, 093004 (2018).
[10] Y. K. Hsiao, Q. Yi, S. T. Cai, and H. J. Zhao, Eur. Phys. J. C **80**, 1067 (2020).
[11] M. L. Du, N. Penalva, E. Hernández, and J. Nieves, Phys. Rev. D **106**, 055039 (2022).
[12] A. Ali, G. Kramer, and C. D. Lu, Phys. Rev. D **58**, 094009 (1998).
[13] Y. B. Li *et al.* (Belle Collaboration), Phys. Rev. Lett. **122**, 082001 (2019).
[14] Y. Li *et al.* (Belle Collaboration), Phys. Rev. D **105**, L011102 (2022).
[15] M. Ablikim *et al.* (BESIII Collaboration), Chin. Phys. C **44**, 040001 (2020).
[16] Q. A. Zhang, J. Hua, F. Huang, R. Li, Y. Li, C. Lü, P. Sun, W. Sun, W. Wang, and Y. Yang, Chin. Phys. C **46**, 011002 (2022).
[17] S. Meinel, Phys. Rev. D **97**, 034511 (2018).
[18] H. Bahtiyar, Turk. J. Phys. **45**, 4 (2021).
[19] H. Bahtiyar, K. U. Can, G. Erkol, M. Oka, and T. T. Takahashi, Phys. Lett. B **772**, 121 (2017).
[20] S. Meinel and G. Rendon, Phys. Rev. D **103**, 094516 (2021).
[21] S. Meinel and G. Rendon, Phys. Rev. D **105**, 054511 (2022).
[22] T. M. Aliev, S. Bilmis, and M. Savci, Phys. Rev. D **104**, 054030 (2021).
[23] Z. X. Zhao, Chin. Phys. C **42**, 093101 (2018).
[24] Z. X. Zhao, arXiv:2103.09436.
[25] Y. L. Liu and M. Q. Huang, J. Phys. G **37**, 115010 (2010).
[26] C. F. Li, Y. L. Liu, K. Liu, C. Y. Cui, and M. Q. Huang, J. Phys. G **44**, 075006 (2017).
[27] P. Guo, H. W. Ke, X. Q. Li, C. D. Lu, and Y. M. Wang, Phys. Rev. D **75**, 054017 (2007).
[28] C. Q. Geng, Y. K. Hsiao, C. W. Liu, and T. H. Tsai, Phys. Rev. D **97**, 073006 (2018).
[29] J. Zou, F. Xu, G. Meng, and H. Y. Cheng, Phys. Rev. D **101**, 014011 (2020).
[30] Y. J. Shi, W. Wang, Y. Xing, and J. Xu, Eur. Phys. J. C **78**, 56 (2018).
[31] F. Huang, Z. P. Xing, and X. G. He, J. High Energy Phys. 03 (2022) 143; 09 (2022) 87.
[32] W. Wang, Z. P. Xing, and J. Xu, Eur. Phys. J. C **77**, 800 (2017).
[33] F. Huang, J. Xu, and X. R. Zhang, Eur. Phys. J. C **81**, 976 (2021).
[34] C. D. Lü, W. Wang, and F. S. Yu, Phys. Rev. D **93**, 056008 (2016).
[35] Y. K. Hsiao, Y. L. Wang, and H. J. Zhao, J. High Energy Phys. 09 (2022) 035.
[36] X. G. He and G. N. Li, Phys. Lett. B **750**, 82 (2015).
[37] C. Q. Geng, C. W. Liu, T. H. Tsai, and S. W. Yeh, Phys. Lett. B **792**, 214 (2019).
[38] H. Y. Cheng, C. W. Chiang, and A. L. Kuo, Phys. Rev. D **91**, 014011 (2015).
[39] K. K. Sharma and R. C. Verma, Phys. Rev. D **55**, 7067 (1997).
[40] M. J. Savage and R. P. Springer, Phys. Rev. D **42**, 1527 (1990).
[41] R. Chistov *et al.* (Belle Collaboration), Phys. Rev. D **88**, 071103 (2013).
[42] S. B. Yang *et al.* (Belle Collaboration), Phys. Rev. Lett. **117**, 011801 (2016).
[43] Y. B. Li *et al.* (Belle Collaboration), Phys. Rev. Lett. **127**, 121803 (2021).
[44] X. G. He, F. Huang, W. Wang, and Z. P. Xing, Phys. Lett. B **823**, 136765 (2021).
[45] M. Ablikim *et al.* (BESIII Collaboration), Chin. Phys. C **39**, 093001 (2015).
[46] M. Ablikim *et al.* (BESIII Collaboration), Phys. Rev. Lett. **116**, 052001 (2016).
[47] M. Ablikim *et al.* (BESIII Collaboration), Phys. Rev. Lett. **129**, 231803 (2022).
[48] M. Ablikim *et al.* (BESIII Collaboration), Phys. Rev. D **108**, L031105 (2023).
[49] R. Aaij *et al.* (LHCb Collaboration), Phys. Rev. Lett. **118**, 182001 (2017).
[50] R. Aaij *et al.* (LHCb Collaboration), Phys. Rev. Lett. **124**, 222001 (2020).
[51] J. Ryżka (LHCb Collaboration), Acta Phys. Pol. B Proc. Suppl. **16**, 12 (2023).
[52] R. Aaij *et al.* (LHCb Collaboration), J. High Energy Phys. 07 (2023) 228.
[53] R. Aaij *et al.* (LHCb Collaboration), arXiv:2305.06711.
[54] A. J. Buras, arXiv:hep-ph/9806471.
[55] Z. P. Xing and Z. X. Zhao, Phys. Rev. D **98**, 056002 (2018).
[56] X. H. Hu, R. H. Li, and Z. P. Xing, Eur. Phys. J. C **80**, 320 (2020).
[57] Z. X. Zhao, arXiv:2204.00759.
[58] W. Wang and Z. P. Xing, Phys. Lett. B **834**, 137402 (2022).
[59] H. Liu, Z. P. Xing, and C. Yang, Eur. Phys. J. C **83**, 123 (2023).
[60] H. W. Ke, N. Hao, and X. Q. Li, Eur. Phys. J. C **79**, 540 (2019).
[61] G. Li, F. l. Shao, and W. Wang, Phys. Rev. D **82**, 094031 (2010).
[62] R. C. Verma, J. Phys. G **39**, 025005 (2012).
[63] Y. J. Shi, W. Wang, and Z. X. Zhao, Eur. Phys. J. C **76**, 555 (2016).
[64] Z. Ghalenovi, C. P. Shen, and M. Moazzen Sorkhi, Phys. Lett. B **834**, 137405 (2022).
[65] R. L. Workman *et al.* (Particle Data Group), Prog. Theor. Exp. Phys. **2022**, 083C01 (2022).
[66] H. Y. Cheng and Y. L. Shi, Phys. Rev. D **98**, 113005 (2018).
[67] V. V. Kiselev and A. K. Likhoded, Phys. Usp. **45**, 455 (2002).
[68] C. G. Boyd, B. Grinstein, and R. F. Lebed, Phys. Rev. D **56**, 6895 (1997).
[69] I. Caprini, L. Lellouch, and M. Neubert, Nucl. Phys. **B530**, 153 (1998).

[70] C. Bourrely, I. Caprini, and L. Lellouch, Phys. Rev. D **79**, 013008 (2009); **82**, 099902(E) (2010).
[71] A. Bharucha, T. Feldmann, and M. Wick, J. High Energy Phys. 09 (2010) 090.
[72] H. Y. Cheng and B. Tseng, Phys. Rev. D **58**, 094005 (1998).
[73] A. Ali and C. Greub, Phys. Rev. D **57**, 2996 (1998).
[74] S. Y. Yu, X. W. Kang, and V. O. Galkin, Front. Phys. (Bejing) **18**, 64301 (2023).
[75] H. Y. Cheng, X. W. Kang, and F. Xu, Phys. Rev. D **97**, 074028 (2018).
[76] Y. S. Dai, D. S. Du, X. Q. Li, Z. T. Wei, and B. S. Zou, Phys. Rev. D **60**, 014014 (1999).
[77] H. Y. Cheng, C. K. Chua, and A. Soni, Phys. Rev. D **71**, 014030 (2005).
[78] M. Beneke, G. Buchalla, M. Neubert, and C. T. Sachrajda, Nucl. Phys. **B606**, 245 (2001).